

Configuration-dependent hybridization in electron spectroscopies of Ce-based compounds

N. Witkowski, F. Bertran, and D. Malterre

*Laboratoire de Physique des Matériaux, Université Henri Poincaré, Nancy I - Boîte Postale 239,
F-54506 Vandœuvre-lès-Nancy, France*

(Received 21 July 1997)

In this paper, we analyze Ce $3d$ core-level photoemission and inverse-photoemission spectra in the framework of the single-impurity Anderson model. We show that the Gunnarsson-Schönhammer model generally used to describe spectroscopic properties of Ce-based systems cannot account for the description of core-hole photoemission and inverse-photoemission spectra with the same set of parameters. By introducing $4f$ configuration-dependent hybridization terms, the situation is significantly improved, and a satisfactory agreement between experimental and calculated spectra is obtained. This result shows that, in contrast to what was previously claimed for highly hybridized compounds, the spectroscopic data of cerium compounds can be described in the framework of the single-impurity Anderson model. [S0163-1829(97)06047-5]

I. INTRODUCTION

Cerium, the first element of the rare-earth series, exhibits some very singular properties, like the pressure-induced isostructural γ -Ce \rightarrow α -Ce phase transition, due to its $4f$ states. Two extreme alternative approaches can be used to describe the $4f$ electrons: band formalism and model Hamiltonians based on localized $4f$ states. In the band description,¹ the $4f$ states form a narrow band, and the γ - α transition is associated with a Mott transition without any significant change of the $4f$ occupation number.² This band formalism leads to a satisfactory description of the thermodynamic properties.³⁻⁵ In the opposite approach, the $4f$ electrons are considered to be localized and weakly coupled, with an itinerant conduction band. Cerium atoms in cerium metal or compounds can be considered as a set of independent impurities, and can be described in the single-impurity Anderson model.⁶ In this framework, the γ - α transition corresponds to a Kondo volume collapse and to an increase of the hybridization between $4f$ and conduction states.⁷ In contrast to the band description, this model emphasizes the role of the electronic correlation between $4f$ states, and suggests the existence of a low-energy scale (the Kondo energy) which is clearly revealed by magnetic susceptibility and neutron inelastic scattering.⁸

High-energy spectroscopies like photoemission or x-ray-absorption spectroscopy (XAS) show satellite structures which can be associated with correlation energy, and then favor a description in terms of strongly correlated localized $4f$ states. The single-impurity Anderson model seems well suited to account for spectroscopic measurements.⁹ For core-hole spectroscopies, Gunnarsson and Schönhammer (GS) proposed to modify the Anderson Hamiltonian to account for the interaction between the $4f$ states and the core-hole created by the photoelectric process.¹⁰ A qualitatively correct description of the photoemission or $M_{4,5}$ XAS results in cerium-based systems is then obtained.¹¹⁻¹⁵ In a systematic study, Allen *et al.* showed that the GS model can reproduce, with the same parameters, $4f$ photoemission, $3d$ photoemission ($3d$ XPS), and bremsstrahlung isochromat spectroscopy (BIS) spectra on several Ce-TM (transition-metal) compounds.¹⁶

Nevertheless, recent results obtained on strongly hybridized systems [CeRh₃,^{17,18} CeIr₂,¹⁹ and Laves phases CeTM₂ (Ref. 18)] have shown some limitations of the GS model. In these systems, the GS model fails to reproduce BIS spectra which mainly present one structure near the Fermi level, and it has been claimed that a description in a band-structure approach would be more suitable than in the localized impurity model. Indeed, the band description allows to account for interactions between neighboring sites which seem to be important in such materials, and are neglected in the localized impurity model. Nevertheless, this question remains very controversial.^{20,21}

In a theoretical point of view, Gunnarsson and Jepsen²² showed, from *ab initio* calculations, that the hybridization coupling depends on the $4f$ configuration. Then they proposed a prescription to account for this effect simply: an effective hybridization has to be introduced for each spectroscopic technique. Recent XAS results obtained on several Ce-Rh compounds and on CeCo₂ (Ref. 15) and BIS results on CeRh₃ (Ref. 21) corroborate this idea of a configuration-dependent hybridization.

However, the difficulties are not restricted to strongly hybridized materials, and we will show in Sec. III A that it is not possible to correctly reproduce BIS results on weakly hybridized compounds with the parameters obtained from the $3d$ XPS analysis. This cannot lead to calling the localized impurity description of the $4f$ states into question, since a band description seems inconceivable for the weakly hybridized compounds. Then improvements of the localized impurity model have to be considered for a good description of the various spectroscopies on both strongly and weakly hybridized systems.

In this paper, we analyze previously published $3d$ XPS and BIS experimental results obtained on CeRu₂,²³ CeRh₃,²⁴ CeNi₂,^{25,26} CePd₃,^{27,11} CeNi,^{25,26} CeSi₂,²⁸ and Ce₇Ni₃ (Refs. 25 and 26) compounds in a modified localized impurity Gunnarsson-Schönhammer model with hybridization terms depending on the $4f$ configuration. The purpose of this work is then to show that, if this dependence is accounted for, one can describe very accurately the $3d$ XPS results as

well as the BIS results on both strongly and weakly hybridized systems.

The paper is organized as follows: in Sec. II, we recall the GS model and introduce the changes in the Hamiltonian due to configuration-dependent parameters. Then, in Sec. III A, we compare XPS and BIS experimental results with the GS calculated spectra, and discuss the observed disagreement. In Sec. III B, we clearly show that a better description is obtained when configuration-dependent hybridizations are used.

II. DESCRIPTION OF THE MODEL

The model generally used to describe spectroscopic properties of Ce compounds is based on the GS Hamiltonian. It results from the Anderson Hamiltonian with an additional term accounting for the interaction between the $4f$ states and the core hole created in the photoelectric process:

$$H_{\text{GS}} = \sum_{k,\sigma} \epsilon_k n_{k,\sigma} + \sum_{m,\sigma} \epsilon_f n_{m,\sigma} + \frac{U_{ff}}{2} \sum_{\substack{m,\sigma \\ m',\sigma'}} n_{m,\sigma} n_{m',\sigma'} \\ + \sum_{k,m,\sigma} (V_{k,m} a_{m,\sigma}^\dagger a_k + \text{H.c.}) \\ - (1 - n_c) U_{fc} \sum_{m,\sigma} n_{m,\sigma} + \epsilon_c,$$

where ϵ_f is the energy of the $4f$ states, $n_{m,\sigma}$ the number of $4f$ electrons in the m, σ state, U_{ff} the Coulomb energy between the $4f$ electrons, $V_{k,m}$ the hybridization between $4f$ and conduction states, $a_{m,\sigma}^\dagger$ the operator creating one $4f$ electron in the m, σ state, a_k the operator destructing one conduction electron, n_c the core-hole occupation, U_{fc} the Coulomb energy between the core-hole and the $4f$ states, and ϵ_c the core-hole energy.

Considering a conduction band discretized in a limited number of states, Jo and Kotani proposed a direct diagonalization method in a restricted basis built from three relevant $4f$ configuration states.²⁹ The diagonalization of H_{GS} in this restricted basis gives the ground and final states associated with the different spectroscopies. The ground state and XPS final states are expressed on $4f^0$, $4f^1$, and $4f^2$ configurations, while the BIS final states are represented on $4f^1$, $4f^2$, and $4f^3$ configurations, since this technique corresponds to the addition of one $4f$ electron. Therefore, the spectral densities exhibit several structures whose intensity corresponds to the matrix elements between the initial and final states of the relevant transition operator, as described in details in Refs. 10, 12 and 30.

This model assumes that the hybridization parameters $V_{k,m}$ do not depend on the number of $4f$ electrons. Gunnarsson and Jepsen have shown from an *ab initio* calculation that the hybridization strength between $4f$ and conduction states is explicitly $4f$ configuration dependent: for Ce metal, a change by a factor of about 0.7 is predicted between the $4f^0$ and $4f^1$ configurations.²² Because of the hybridization terms, initial and final states are not pure, but result mainly from a mixing of two configurations. Then these authors show that one has to consider the hybridization coupling corresponding to the higher occupation of the configuration mixture (e.g.,

$4f^1$ in the ground state, since it is a $4f^0$ and $4f^1$ configuration mixture). Therefore, since three configurations are involved in the calculation of the ground and final states, two hybridization parameters should be introduced in the Hamiltonian. To simplify the problem, Gunnarsson and Jepsen proposed a prescription: an effective hybridization can be used for each technique, and its value has to be associated with the dominant configuration in the final state (i.e., $4f^2$ for core-level XPS and BIS). This method was recently successfully applied to the interpretation of BIS and XPS spectra of CeRh₃.²⁴ Thanks to this modification of the single-impurity Anderson model, the experimental results have been correctly described, while it was claimed that this model was unable to describe the properties of strongly hybridized systems like CeRh₃.^{17,18} However, calculations can be directly carried out with configuration-dependent hybridizations. This has been done for resonant inverse photoemission on CeNi₂,³¹ Cu $2p$ photoemission on Sr₂CuO₃,³² and for Ni $2p$ photoemission on NiCl₂.³³ The hybridization strengths associated with the different $4f$ configurations should be considered as free parameters, but their evolution satisfies systematic trends. First, the increase in the $4f$ occupation number yields a larger wave-function spatial extension and, as confirmed in the *ab initio* calculations of Gunnarsson and Jepsen, a larger hybridization. Second, when a core hole is created, the $4f$ states are localized by the attractive core-hole potential leading to a decrease in the hybridization strength.

To describe the ground state, we have to introduce two hybridization parameters: V_1^g for the $4f^0$ - $4f^1$ coupling, and V_2^g for the $4f^1$ - $4f^2$ coupling. The ratio $R = V_1^g/V_2^g$ is lower than unity, because V_2^g corresponds to a larger $4f$ occupation. For the final states of core-level photoemission, we define two final-state hybridization parameters V_1^{XPS} and V_2^{XPS} for $c4f^0$ - $c4f^1$ and $c4f^1$ - $c4f^2$ couplings, respectively (c denotes the core hole) satisfying $V_1^{\text{XPS}}/V_2^{\text{XPS}} = R$. As discussed above, $V_1^{\text{XPS}} \leq V_1^g$ due to the core-hole-induced $4f$ localization. The hybridization parameters for the final states of the inverse photoemission are V_2^{BIS} and V_3^{BIS} for the $4f^1$ - $4f^2$ and $4f^2$ - $4f^3$ couplings, respectively, with $V_2^{\text{BIS}} = V_2^g$ since there is no core hole in the final state of BIS. Moreover, we impose $V_2^{\text{BIS}}/V_3^{\text{BIS}} = R$. Finally, we used different values of the Coulomb interaction between $4f$ electrons in the ground and final states of photoemission with, in principle, $U_{ff}^{\text{fin}} > U_{ff}^g$, since the $4f$ state localization due to the core hole should lead to an increase in the interaction between $4f$ electrons.

In the following calculations, we used a rectangular conduction band (4 eV wide, and discretized in ten states). The XPS spectra are convoluted with a Lorentzian (the full width at half maximum FWHM is equal to 1 eV) accounting for the core-hole lifetime, and with a Gaussian (varying FWHM) simulating experimental resolution and multiplet effects. The spectra are then duplicated with a 18.6-eV shift, and with a $\frac{3}{2}$ intensity factor to obtain the $3d_{5/2}$ component. Finally, a Shirley background was added to simulate inelastic backgrounds. In the case of BIS, the spectra are convoluted with a FWHM equal to 0.2 eV Lorentzian, and a FWHM equal to 1 eV Gaussian for the structure near the Fermi edge. The structure at higher energy is convoluted with a larger Gaussian (the FWHM is equal to 3–4 eV) in order to account

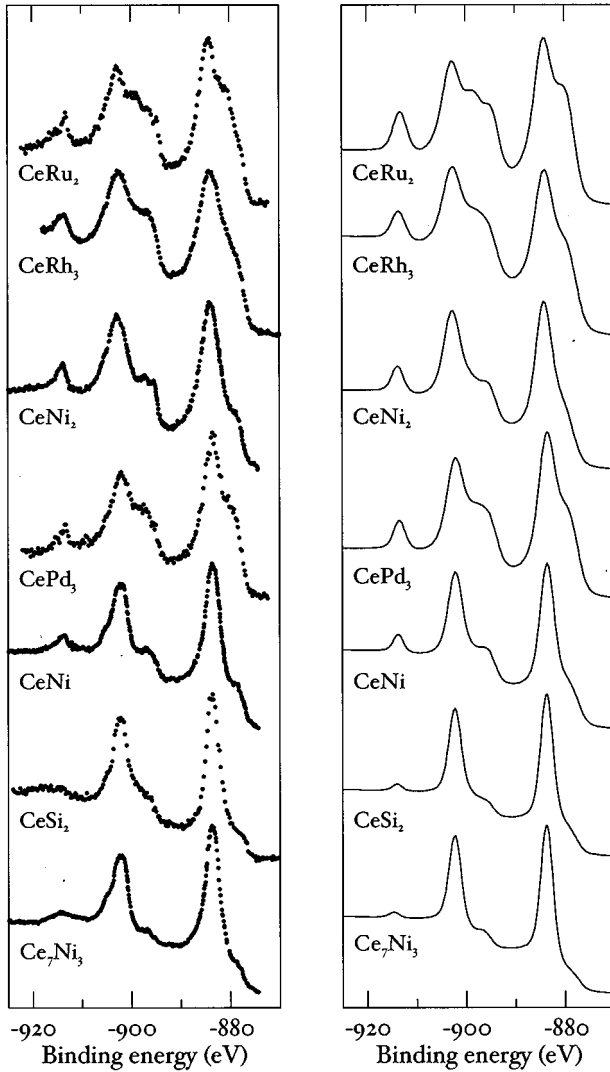


FIG. 1. Ce 3d XPS experimental spectra (dots) and calculated spectra in the Gunnarsson-Schönhammer model framework (line).

artificially for the broadening due to multiplet effects. An arctan background has been added to simulate the transitions toward delocalized $5d6s$ states and, in the case of CeRh_3 and CePd_3 , a contribution due to the Ce $5d$ split-off band³⁴ is also added to the calculated spectra.²⁷

III. RESULTS

A. Limitations of the Gunnarsson-Schönhammer model

First, we would like to demonstrate that the GS model, in its standard form, cannot account for core-level XPS and BIS with the same set of parameters. This behavior, previously shown in the case of strongly hybridized systems,¹⁷ is also encountered in weakly hybridized systems. We then performed a simulation of experimental Ce $3d$ XPS spectra, in the GS model framework, for a series of compounds chosen for their different configuration mixing. In Fig. 1, we compare the experimental and calculated spectra, and Table I summarizes the parameters we used. It should be noted that the energy scale of the CeRh_3 experimental spectrum has been adjusted to the other ones, since the spectrum presented in Ref. 24 is largely shifted. The structure intensities as well as their energy positions are correctly reproduced, and the agreement between experimental and calculated spectra is very satisfactory. XPS spectra are composed, in each spin-orbit contribution, of three structures corresponding, respectively, to transitions toward final states with mainly $4f^0$, $4f^1$, and $4f^2$ characters (in increasing kinetic-energy order). The intensity of the so-called $4f^0$ structure is related to the $4f^0-4f^1$ configuration mixture in the initial state, while the intensity of the so-called $4f^2$ one results mainly from the $4f^1-4f^2$ configuration mixture in the final state.

With the parameters used for XPS spectra, we then calculated the BIS spectra. Corresponding to the addition of one $4f$ electron, BIS spectra exhibit two structures associated with final states of mainly $4f^1$ and $4f^2$ characters. In the case of CeRh_3 and CePd_3 , a third structure can be observed around 2–3 eV. It results from transitions toward the Ce $5d$ split-off band. Obviously, the GS calculations cannot take into account such transitions and, in our calculation, the structure has been artificially added to the background. It should be noted that the background then obtained for CePd_3 is similar to the YPd_3 spectra.³⁴ Several disagreements between experimental and calculated spectra are clearly observed in Fig. 2. On the one hand, the energy separation between the two structures is not quantitatively reproduced. Nevertheless, the systematic increase in the energy position of the high-energy structure observed in the experimental data is also obtained in the calculated spectra. In the zero-hybridization limit, the energy of this $4f^2$ structure is simply $U_{ff} + 2\epsilon_f$. Hybridization will lead to an increase in the en-

TABLE I. Gunnarsson-Schönhammer model parameter values used to reproduce experimental spectra.

	Ground state			BIS final state	XPS final state	
	U_{ff} (eV)	ϵ_f (eV)	V (eV)	$4f^2$ struct. weight	U_{fc} (eV)	$4f^0$ struct. weight
CeRu ₂	7.0	−1.25	0.45	57.1 %	10.0	16.0 %
CeRh ₃	7.0	−1.4	0.43	62.7 %	10.2	13.8 %
CeNi ₂	6.8	−1.2	0.35	69.4 %	10.3	13.6 %
CePd ₃	7.5	−1.5	0.41	68.0 % ^a	10.5	12.3 %
CeNi	6.8	−1.4	0.33	77.2 %	10.6	9.7 %
CeSi ₂	6.8	−1.6	0.27	88.6 % ^b	10.4	4.6 %
Ce ₇ Ni ₃	6.8	−1.6	0.25	90.7 %	10.95	3.9 %

^a20-K measurement.

^b15-K measurement.

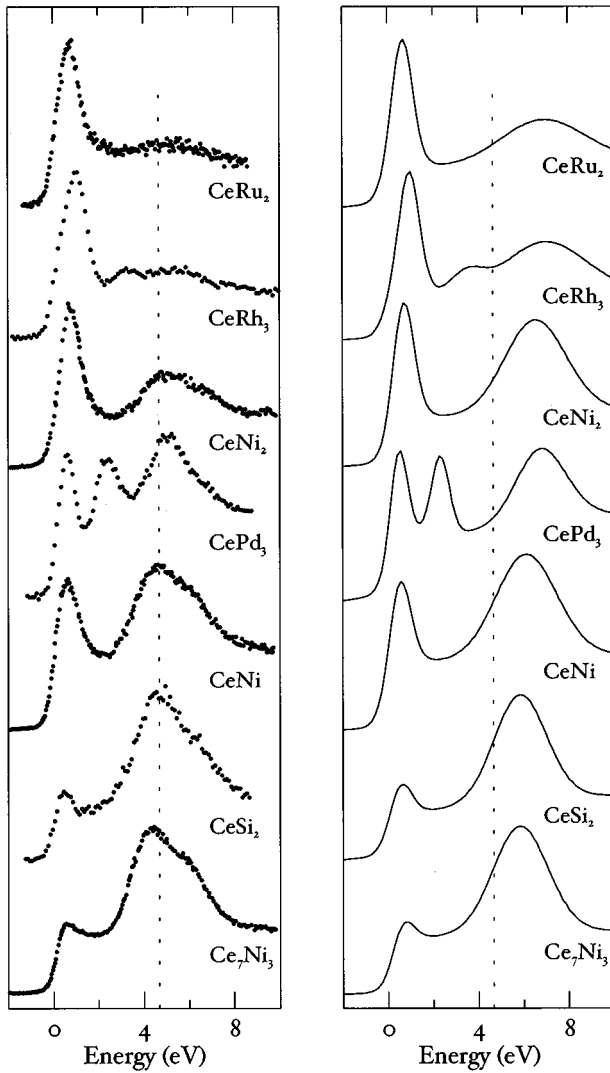


FIG. 2. BIS experimental spectra (dots) and calculated spectra in the Gunnarsson-Schönhammer model framework (line).

ergy separation, and then to a shift of the $4f^2$ peak toward higher energy. The disagreement between experiments and calculations suggests that the U_{ff} value, which mainly determines the energy position of the $4f^2$ structure, is overestimated for BIS spectroscopy. As the U_{ff} values we used are deduced from the analysis of XPS spectra, we can deduce that U_{ff} is not the same in BIS and XPS final states, confirming that it depends on the core-level occupation.

Another systematic trend is observed: the $4f^2$ structure weight is too large in the calculated spectra, and this discrepancy increases by going from Ce_7Ni_3 to CeRu_2 . In the GS model, the weight of this structure is related to the configuration mixture in the initial state, i.e., to the hybridization V : the larger the configuration mixture, the larger the $4f^1$ structure weight, and then the smaller the $4f^2$ structure weight is. In the standard GS model, the same V is used in the calculation of the ground state and XPS final states. Thus it is underestimated for the ground state, and yields too large a $4f^2$ structure weight in the BIS spectra.

Finally, we would like to point out that as the GS model gives zero-temperature spectral functions, whereas the experimental spectra are usually obtained at room temperature.

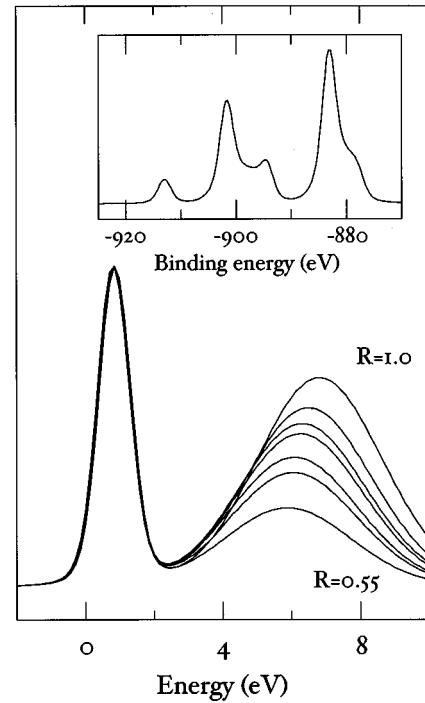


FIG. 3. Calculated BIS spectra with different values of the hopping term ratio R (0.55, 0.60, 0.62, 0.65, 0.70, 0.80, and 1.0). The corresponding XPS spectra are identical whatever the value of R , and one of them is shown in the inset.

A disagreement between zero-temperature calculations and room-temperature measurements could result from the temperature-dependence of the spectral function. Recent BIS measurements on CePd_3 and CeSi_2 (Refs. 27 and 28) actually exhibit a small temperature dependence between 15 and 300 K, whereas no dependence was observed in strongly hybridized materials like CeNi_2 .³⁵ The CePd_3 and CeSi_2 spectra reported in Fig. 2 correspond to low-temperature measurements ($T=20$ and 15 K), and then the observed disagreement cannot be explained by temperature effects.

B. Results of configuration-dependent hybridization calculations

We would like to demonstrate now that, when configuration-dependent hybridization is taken into account, XPS and BIS spectra can be satisfactorily described in the framework of the single-impurity Anderson model. First, to illustrate the modifications due to configuration-dependent hybridization, we calculated some BIS spectra with several values of the R ratio (Fig. 3). In these calculations, the $4f^0$ configuration weight in the initial state was kept constant as well as the XPS spectrum. All the BIS spectra were normalized to the $4f^1$ structure intensity in order to highlight the $4f^2$ structure evolution.

The first effect of the configuration-dependent hybridization is a decrease of the $4f^2$ structure intensity. With increasing $4f^1$ - $4f^2$ hybridization (i.e., decreasing R), the weight of the $4f^2$ configuration increases in the ground state, and decreases in the final states corresponding to the so-called $4f^2$ structure. Therefore, the transition probability between the initial and final states associated with the $4f^2$ structure de-

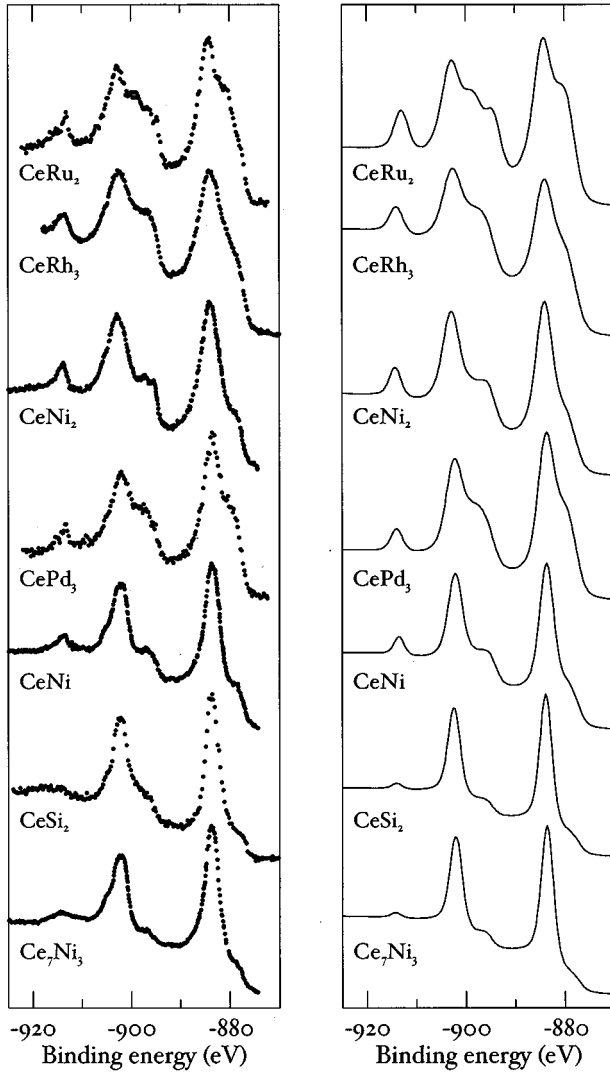


FIG. 4. Ce 3d XPS experimental spectra (dots) and calculated spectra with the configuration-dependent hybridization model (line).

creases. Figure 3 shows that the intensity change is not linear with R , since it varies more slowly when R goes up to unity. The second effect is the modification of the energy separation between $4f^1$ and $4f^2$ structures, which is mainly due to a hybridization-induced energy shift. These effects should lead to a better agreement between experimental and calculated spectra, especially for the strongly hybridized systems.

We have tried to reproduce BIS and XPS experimental spectra of the series of compounds we considered in Sec. III A. In Figs. 4 and 5, we compare the XPS and BIS experimental spectra with simulations obtained in the configuration-dependent hybridization framework. The parameters used in these calculations are summarized in Table II. The two main discrepancies observed in BIS spectra calculated with the GS model concern the energy separation between $4f^1$ and $4f^2$ structures and the $4f^2$ structure intensity. First, the energy separation between the two structures is now correct owing to the introduction of a larger Coulomb energy for configurations with a core hole. Therefore, a $U_{ff}^g \sim 5$ eV value is involved in the ground and BIS final states whereas a larger value ($U_{ff}^{XPS} \sim 6-7$ eV) is found for

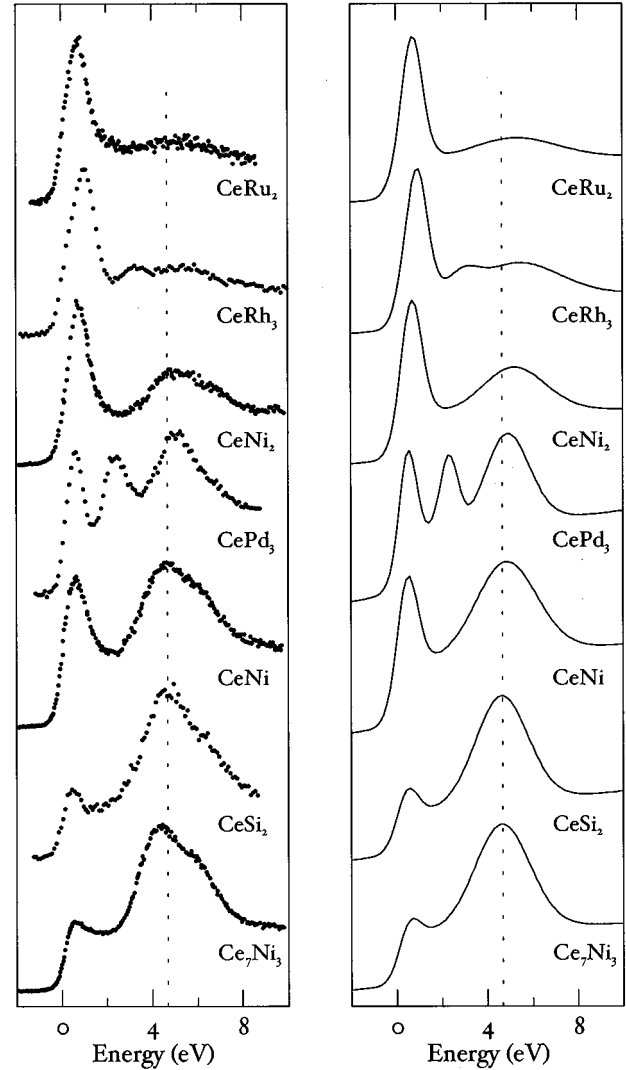


FIG. 5. BIS experimental spectra (dots) and calculated spectra with the configuration-dependent hybridization model (line).

XPS final states, reflecting the $4f$ localization due to the core-hole potential. The U_{ff}^g is in good agreement with the value calculated by Herbst, Watson, and Wilkins³⁶ in the renormalized atom model.

Second, the calculated BIS $4f^2$ structure intensity is in good agreement with experiments especially for strongly hybridized systems, where the discrepancy is important in the GS model. This behavior is directly related to the introduction of $4f$ configuration-dependent hybridization parameters, as demonstrated in Fig. 3. When the configuration mixture is small (CeSi₂ and Ce₇Ni₃), R is close to unity, which means that the hybridization strength is weakly influenced by the $4f$ configuration. On the contrary, when the configuration mixture is larger (CeRu₂ and CeRh₃), the $4f$ configuration strongly influences the hybridization strength and the calculated BIS $4f^2$ structure intensity is significantly smaller than that obtained from the GS model. We would like to point out that the value we obtained for R (0.65–0.70) is in good agreement with the value estimated for α -Ce by Gunnarsson and Jepsen²² from *ab initio* calculations. Finally, a systematic decrease of the $4f$ state energy $|\epsilon_f|$ is observed between Ce₇Ni₃ and CeRu₂, as within the GS model calculations.

TABLE II. Configuration-dependent hybridization model parameter values used to reproduce experimental spectra. $R = V_1^g/V_2^g = V_1^{\text{XPS}}/V_2^{\text{XPS}}$.

	Ground state				BIS final state		XPS final state		
	U_{ff}^g (eV)	ϵ_f (eV)	V_1^g (eV)	R	$4f^2$ struct. weight	U_{ff}^{fin} (eV)	U_{fc} (eV)	V_1^{XPS} (eV)	$4f^0$ struct. weight
CeRu ₂	5.0	-0.9	0.48	0.66	39.5%	5.6	9.8	0.22	15.7%
CeRh ₃	5.3	-1.1	0.43	0.65	49.6%	6.8	10.8	0.20	13.7%
CeNi ₂	5.5	-1.2	0.43	0.64	51.5%	6.3	10.5	0.13	13.6%
CePd ₃	5.5	-1.2	0.33	0.67	68.5% ^a	7.5	11.0	0.23	9.8%
CeNi	5.5	-1.2	0.31	0.68	72.3%	6.3	10.5	0.16	9.7%
CeSi ₂	5.5	-1.4	0.23	0.90	89.4% ^b	6.0	10.4	0.23	4.0%
Ce ₇ Ni ₃	5.5	-1.4	0.22	0.95	90.8%	6.6	10.95	0.22	3.7%

^a20-K measurement.

^b15-K measurement.

This evolution is related to the variation of the ground-state configuration mixing. Comparison of Figs. 2 and 5 clearly demonstrates that configuration-dependent hybridizations have to be used for correctly describing both XPS and BIS results, especially on strongly hybridized systems.

IV. CONCLUSION

In this paper, we carried out a systematic study of core-level XPS and BIS spectra of cerium compounds in the framework of the single-impurity Anderson model. We clearly demonstrated that XPS and BIS cannot be simulated with the same set of parameters: if the XPS spectra are correctly reproduced, disagreements on the energy separation and intensity are observed for the BIS features. Then, following a suggestion of Gunnarsson and Jepsen, we modified the

GS model to take into account the configuration dependence of the hybridization terms, and also introduced a modification of the correlation energy U_{ff} in the presence of a core hole. A very good description was then obtained, even for strongly hybridized materials, for which it was claimed that a band description would be more suitable. The single-impurity Anderson model seems to contain the main physical ingredients to describe the spectroscopic properties of cerium-based compounds, confirming that electronic correlations play the fundamental role in these materials.

ACKNOWLEDGMENT

Laboratoire de Physique des Matériaux is Unité Mixte de Recherche No. 7556 du Centre National de la Recherche Scientifique.

- ¹See, e.g., W. E. Pickett, A. J. Freeman, and D. D. Koelling, Phys. Rev. B **23**, 1266 (1981); A. R. Mackintosh, Physica B **130**, 112 (1985).
- ²B. Johansson, Philos. Mag. **30**, 469 (1974).
- ³O. Eriksson, R. C. Albers, A. M. Boring, G. W. Fernando, Y. G. Hao, and B. R. Cooper, Phys. Rev. B **43**, 3137 (1991).
- ⁴Z. Szotek, W. M. Temmerman, and H. Winter, Phys. Rev. Lett. **72**, 1244 (1994).
- ⁵A. Svane, Phys. Rev. Lett. **72**, 1248 (1994).
- ⁶P. W. Anderson, Phys. Rev. **124**, 41 (1961).
- ⁷J. W. Allen and R. M. Martin, Phys. Rev. Lett. **49**, 1106 (1982).
- ⁸A. P. Murani, Z. A. Bowden, A. D. Taylor, R. Osborn, and W. G. Marshall, Phys. Rev. B **48**, 13 981 (1993).
- ⁹Y. Baer and W.-D. Schneider, in *Handbook on the Physics and Chemistry of Rare Earths*, edited by K. A. Gschneidner, Jr., L. Eyring, and S. Hüfner (North-Holland, Amsterdam, 1987), Vol. 10, p. 1.
- ¹⁰O. Gunnarsson and K. Schönhammer, Phys. Rev. Lett. **50**, 604 (1983); Phys. Rev. B **28**, 4315 (1983).
- ¹¹E. Wuilloud, H. R. Moser, W.-D. Schneider, and Y. Baer, Phys. Rev. B **28**, 7354 (1983).
- ¹²A. Kotani, T. Jo, and J. C. Parlebas, Adv. Phys. **37**, 37 (1988).
- ¹³L. Z. Liu, J. W. Allen, O. Gunnarsson, N. E. Christensen, and O. K. Andersen, Phys. Rev. B **45**, 8934 (1992); J. W. Allen and L. Z. Liu, *ibid.* **46**, 5047 (1992).
- ¹⁴C. Laubschat, E. Weschke, C. Holtz, M. Domke, O. Strebel, and G. Kaindl, Phys. Rev. Lett. **65**, 1639 (1990).
- ¹⁵P. Vavassori, L. Duò, G. Chiaia, M. Qvarford, and I. Lindau, Phys. Rev. B **52**, 16 503 (1995).
- ¹⁶J. W. Allen, S. J. Oh, O. Gunnarsson, K. Schönhammer, M. B. Maple, M. S. Torikachvili, and I. Lindau, Adv. Phys. **35**, 275 (1986).
- ¹⁷E. Weschke, C. Laubschat, R. Ecker, A. Höhr, M. Domke, G. Kaindl, L. Severin, and B. Johansson, Phys. Rev. Lett. **69**, 1792 (1992).
- ¹⁸L. Severin and B. Johansson, Phys. Rev. B **50**, 17 886 (1994).
- ¹⁹C. Laubschat, E. Weschke, M. Domke, C. T. Simmons, and G. Kaindl, Surf. Sci. **269/270**, 605 (1992).
- ²⁰D. Malterre, M. Grioni, Y. Baer, L. Braicovich, L. Duò, P. Vavassori, and G. L. Olcese, Phys. Rev. Lett. **73**, 2005 (1994); E. Weschke, C. Laubschat, A. Höhr, M. Domke, G. Kaindl, L. Severin, and B. Johansson, *ibid.* **73**, 2006 (1994).
- ²¹L. Braicovich, L. Duò, P. Vavassori, D. Malterre, M. Grioni, Y. Baer, and G. L. Olcese, Physica B **206&207**, 77 (1995).
- ²²O. Gunnarsson and O. Jepsen, Phys. Rev. B **38**, 3568 (1988).
- ²³E. Wuilloud, Y. Baer, and M. B. Maple, Phys. Lett. A **97**, 65 (1983).
- ²⁴L. Duò, P. Vavassori, L. Braicovich, N. Witkowski, D. Malterre, M. Grioni, Y. Baer, and G. Olcese, Z. Phys. B **103**, 63 (1997).

- ²⁵F. U. Hillebrecht, J. C. Fuggle, G. A. Sawatzky, M. Campagna, O. Gunnarsson, and K. Schönhammer, *Phys. Rev. B* **30**, 1777 (1984).
- ²⁶J. C. Fuggle, F. U. Hillebrecht, Z. Zolnierak, R. Lässer, Ch. Freiburg, O. Gunnarsson, and K. Schönhammer, *Phys. Rev. B* **27**, 7330 (1983).
- ²⁷D. Malterre, M. Grioni, P. Weibel, B. Dardel, and Y. Baer, *Phys. Rev. Lett.* **68**, 2656 (1992).
- ²⁸D. Malterre, M. Grioni, P. Weibel, B. Dardel, and Y. Baer, *Europhys. Lett.* **20**, 445 (1992).
- ²⁹T. Jo and A. Kotani, *Solid State Commun.* **54**, 451 (1985); *J. Phys. Soc. Jpn.* **55**, 2457 (1986).
- ³⁰J.-M. Imer and E. Wuilloud, *Z. Phys. B* **66**, 153 (1987).
- ³¹K. Tanaka and T. Jo, *Physica B* **206&207**, 74 (1995).
- ³²K. Okada and A. Kotani, *J. Electron Spectrosc. Relat. Phenom.* **71**, R1 (1995).
- ³³K. Okada, A. Kotani, K. Maiti, and D. D. Sarma, *J. Phys. Soc. Jpn.* **65**, 1844 (1996).
- ³⁴F. U. Hillebrecht, J. C. Fuggle, G. A. Sawatzky, and R. Zeller, *Phys. Rev. Lett.* **51**, 1187 (1983).
- ³⁵D. Malterre, M. Grioni, and Y. Baer, *Adv. Phys.* **45**, 299 (1996).
- ³⁶J. F. Herbst, R. E. Watson, and J. W. Wilkins, *Phys. Rev. B* **17**, 3089 (1978).